

Core helium burning using turbulent convection models in intermediate and massive stars: Implications for Cepheid models

(Report for the Kavli-MPA project)

Submitted By

Mami Deka

Project supervisors:

Felix Ahlborn, Teresa Braun, and Achim Weiss

October 30, 2023

Abstract

In this report, we present the results of the Kavli-MPA Summer Program in Astrophysics, 2023. Cepheids are radially pulsating, intermediate-mass stars in the core-helium burning phase. The appearance of blue loops in the evolutionary tracks, which are essential for explaining the observed characteristics of Cepheids, cannot always be reproduced for lower mass Cepheids when only using classical, local mixing length theory (MLT). This has been so far achieved through an ad-hoc extension of the MLT for convection. Besides, the long-standing mass discrepancy problem related to Cepheids provides us with a unique opportunity to confront the stellar theories with observations. In this work, we use a non-local turbulent convection model (TCM) which can explain overshooting directly from the solution of the TCM equations. The primary objective of this study is to test the TCM by applying it to core-helium burning stars, particularly to Cepheids, to predict convective boundary mixing and consequently address the “mass discrepancy” problem of Cepheids. We used the state-of-the-art 1D stellar evolution code “GARSTEC” and computed evolutionary tracks for intermediate-mass core-helium burning stars within the mass range of $3 - 10M_{\odot}$. We compare these tracks with those computed with MLT with and without ad-hoc overshooting. To further validate our results against observations, we selected Cepheids in detached binary systems from the literature and computed evolutionary tracks for them. The stellar evolution tracks generated using the TCM and MLT with ad-hoc overshooting exhibit similar appearances. Overshoot mixing from the convective core and the Cepheid blue-loop have been achieved naturally as solutions to the equations of the TCM. For the three binary systems selected, we studied how well the TCM reproduces their observed stellar parameters, including mass (M), luminosity (L/L_{\odot}), radius (R/R_{\odot}) and effective temperature (T_{eff}). We are planning to include more systems before writing a paper. During the program, we have successfully generated Cepheids’ blue loops with a TCM without any fine-tuning of the involved numerical parameters and with overshooting predicted directly from the convection theory. Beyond the achievement of blue loops, our approach has also proven effective in resolving the long-standing “mass discrepancy” problem associated with Cepheids, achieved through a more physical treatment of convection. However, due to time constraints during the Kavli program, we have been able to work only with three systems. In this report, we describe our modeling results for these three systems and the challenges we faced in reproducing the observations.

Key words: Convection - turbulence - stars: evolution - stars: variables: Cepheids

1 Introduction

Convection is one of the most important mechanisms for the transport of energy and chemical elements within stars, profoundly impacting their structure, evolution, and pulsation properties. However, convection within stars is a highly turbulent, non-linear, and time-dependent three-dimensional (3D) phenomenon, resulting in considerable computational demands. Hence, the implementation of 3D turbulent convection into a simplified one-dimensional (1D) evolutionary model is very challenging. In the literature, the prevailing approach for describing convection is the widely adopted Mixing Length Theory (MLT) (Biermann, 1932; Böhm-Vitense, 1958). Nevertheless, MLT is time-independent and localized in nature. It considers the Schwarzschild boundary as rigid, thus falling short in explaining convective motions beyond this boundary. It also does not produce the blue loops in the evolutionary tracks, which are essential to explain the existence of Cepheids. To account for convective overshooting effects in stellar models, different descriptions need to be employed. The influence of convective overshooting on stellar structure can be mimicked by introducing additional mixing at convective boundaries during stellar evolution—a concept we refer to as “ad-hoc overshooting.” For example, the inclusion of ad-hoc overshooting in MLT does produce the Cepheid blue loops. Nonetheless, this approach cannot predict the temperature gradient within the overshooting region or the extent of this region. This underlines the need to incorporate physically more accurate and numerically feasible theories of convection such as a “turbulent convection model” (TCM) into stellar structure and evolutionary theories.

A large number of TCM developed for stellar convection can be found in literature (Xiong, 1978, 1986; Stellingwerf, 1982; Kuhfuß, 1986, 1987; Canuto, 1992, 1993, 1997; Canuto & Dubovikov, 1998; Canuto, 2011; Li & Yang, 2007). These models vary in terms of the chosen variables, approximations, and assumptions (Kupka et al., 2022, and references therein). In our study, we have employed the TCM developed by Kuhfuß (1986, 1987), which has already been integrated into the Garching Stellar Evolution Code (GARSTEC; Weiss & Schlattl, 2008) (Flaskamp, 2003; Kupka et al., 2022; Ahlborn et al., 2022). This model has already undergone thorough validation in the context of intermediate-mass main-sequence stars (Ahlborn et al., 2022). In the present study, we extend its application to intermediate-mass core-helium burning stars.

Cepheids represent a class of intermediate-mass pulsating stars in the core-helium burning phase. They are particularly known because of their period-luminosity relation (PLR), which makes them excellent distance indicators. Besides being crucial distance indicators, Cepheids also provide us with ideal stellar laboratories to test and validate stellar evolutionary and pulsation theories. In this work, we have used Cepheids to test the TCM, more specifically we look into the “Cepheid mass discrepancy” problem (Stobie, 1969; Cox, 1980; Keller, 2008).

The “Cepheid mass discrepancy” problem is a long-standing puzzle in the field of stellar evolutionary and pulsation theories. Nevertheless, this has presented us with a unique opportunity to refine and improve these very theories. The Cepheid’s mass can be determined using both their evolutionary and pulsation properties. However, the Cepheid’s evolutionary mass has been found to be significantly higher than the pulsation mass (Stellingwerf, 1982). Cox (1980) reported this mass discrepancy to be $\sim 40\%$. The improved opacity calculations performed by the OPAL group (Iglesias & Rogers, 1993, 1996) have reduced this discrepancy to $\sim (10 - 20)\%$. Nevertheless, it was not clear whether the evolutionary mass or pulsation mass was correct until recently. Pietrzyński et al. (2010) have for the first time provided the dynamical mass of Cepheids to an accuracy of 1% for the OGLE-LMC-CEP-0227 binary sys-

tem. Their findings indicated consistency between the dynamical mass and the pulsation mass within the margins of error. Hence, the possible solutions for the remaining discrepancy concerns the improvement of the physics of the evolutionary model: convective core overshooting, mass loss, and rotational mixing (Keller, 2008; Neilson et al., 2011; Prada Moroni et al., 2012; Anderson et al., 2014, and references therein). Including these effects in evolutionary models will help us to bring the evolutionary mass and the dynamical mass into agreement. Convective core overshooting during main sequence evolution leads to a more massive post-main sequence helium core, thereby resulting in a more luminous Cepheid for the same mass (Cassisi & Salaris, 2011). While incorporating mass loss during the Cepheid evolution can reduce the stellar mass without affecting the stellar luminosity (Neilson et al., 2011). Furthermore, the inclusion of rotation can also increase the luminosity of the Cepheid without increasing the initial mass (Anderson et al., 2014). The present study focuses on the more physical treatment of convective core overshooting. Our goal is to test the convection theory by Kuhfuß (1986). If significant mismatches with the observations are found, refining and improving the theory will be a consequence of this project.

The remainder of the report is organized as follows: we discuss the computation of stellar models spanning a mass range of $(3 - 10)M_{\odot}$ with the TCM and subsequently compare its results with the overshooting model extended in an ad-hoc manner in Sect. 2. Sect. 3 presents the models for the studied binary systems OGLE-LMC-CEP-0227, OGLE-LMC-CEP-1812, and OGLE-LMC-CEP-4956. Finally, the summary and conclusion are presented in Sect. 4.

2 Stellar evolutionary models with TCM

2.1 The Kuhfuss TCM

We have used the GARSTEC to compute the evolutionary tracks. The TCM by Kuhfuß (1986, 1987) including the non-local terms is already implemented in the GARSTEC (Flaskamp, 2003; Kupka et al., 2022; Ahlborn et al., 2022) and well tested in main-sequence stars with convective cores (Ahlborn et al., 2022). This model encompasses three partial differential equations governing turbulent kinetic energy (ω), convective flux (Π), and entropy fluctuations (Φ), along with enhanced dissipation rates within the overshooting regions. Ahlborn et al. (2022) referred to this model as the 3-equation model (hereafter TCM3). To aid the reader's understanding, we summarize the equations below:

$$d_t \omega = \frac{\nabla_{\text{ad}} T}{H_p} \Pi - \frac{C_D}{\Lambda} \omega^{3/2} - \mathcal{F}_{\omega} \quad (1)$$

$$d_t \Pi = \frac{2\nabla_{\text{ad}} T}{H_p} \Phi + \frac{2c_p}{3H_p} (\nabla - \nabla_{\text{ad}}) \omega - \mathcal{F}_{\Pi} - \frac{1}{\tau_{\text{rad}}} \Pi \quad (2)$$

$$d_t \Phi = \frac{c_p}{H_p} (\nabla - \nabla_{\text{ad}}) \Pi - \mathcal{F}_{\Phi} - \frac{2}{\tau_{\text{rad}}} \Phi \quad (3)$$

here, ∇ and ∇_{ad} represent the model and adiabatic temperature gradient, respectively. The substantial derivative is denoted as $d_t = \partial_t + \vec{v} \cdot \nabla$.

The radiative dissipation timescale is given as

$$\tau_{\text{rad}} = \frac{c_p \kappa \rho^2 \Lambda^2}{4\sigma T^3 \gamma_R^2}.$$

Table 1: The turbulent convection parameter set for the TCM1.

Parameters	Values	Remarks
α_{TCM1}	1.11	Solar calibrated
α_ω	0.3	Ahlborn et al. (2022)
C_D	$\frac{8}{3} \cdot \sqrt{\frac{2}{3}}$	Calibrated to MLT analytically
α_s	$\frac{1}{2} \sqrt{\frac{2}{3}}$	Calibrated to MLT analytically

Non-local fluxes \mathcal{F}_a are modelled as:

$$\mathcal{F}_a = \frac{1}{\bar{\rho}} \operatorname{div} (-\alpha_a \bar{\rho} \Lambda \sqrt{\omega} \nabla \bar{a})$$

for $a = \omega, \Pi, \Phi$.

The number of equations is reduced to one by introducing the following approximation for the convective flux:

$$\Pi = \alpha_s \Lambda \sqrt{\omega} \frac{c_p}{H_p} (\nabla - \nabla_{\text{ad}}). \quad (4)$$

This approximation of the convective flux allows eliminating it from the ω -equation such that it is only necessary to solve a single equation. [Ahlborn et al. \(2022\)](#) refer to this simplified model as the 1-equation model (hereafter TCM1):

$$\frac{\partial \omega}{\partial t} = \frac{\nabla_{\text{ad}} T \Lambda \alpha_s c_p}{H_p^2} \sqrt{\omega} (\nabla - \nabla_{\text{ad}}) - \frac{C_D}{\Lambda} \omega^{\frac{3}{2}} - \mathcal{F}_\omega \quad (5)$$

We have incorporated the TCM1 while computing the evolutionary tracks until the core helium burning phase throughout this paper, as the TCM3 shows numerical convergence issues before reaching the core helium burning phase.

The parameters $C_D, \gamma_R, \alpha_\omega, \alpha_\Pi$, and, α_Φ represent the turbulent convection (TC) parameters. Λ is the length scale of TKE dissipation, which can be expressed by the product of the pressure scale height H_p and a parameter α_{TCM1} , which is analog to the MLT-parameter. The variables T and ρ correspond to the stellar structure variables temperature and density, respectively. To avoid the divergence of the dissipation length-scale Λ for small radii, occurring due to the divergence of the pressure scale height, we further apply a geometric limitation of the dissipation length scale as suggested by [Wuchterl \(1995\)](#). Additionally, c_p denotes the specific heat capacity at constant pressure, κ refers to the Rosseland opacity, and σ to the Stefan-Boltzmann constant. The quantities with a bar are the spherically averaged quantities. For detailed derivations and symbol definitions, we refer the readers to the works of [Kuhfuß \(1986, 1987\)](#); [Flaskamp \(2003\)](#); [Kupka et al. \(2022\)](#); [Ahlborn et al. \(2022\)](#).

The α_{MLT} and α_{TCM1} (in case of TCM1) are determined by a solar calibration. A solar calibration is used to find a model with the same radius, luminosity, and surface metal to hydrogen fraction $\frac{Z_\odot}{X_\odot}$ as the present day sun. A sequence of stellar models with varying initial values of Y, Z and α_{MLT} or α_{TCM1} is calculated and evolved until the age of the sun to find the correct combination of these parameters for a solar model. A solar calibration was done for a model with MLT and a model with the TCM1 using the solar abundances as given by

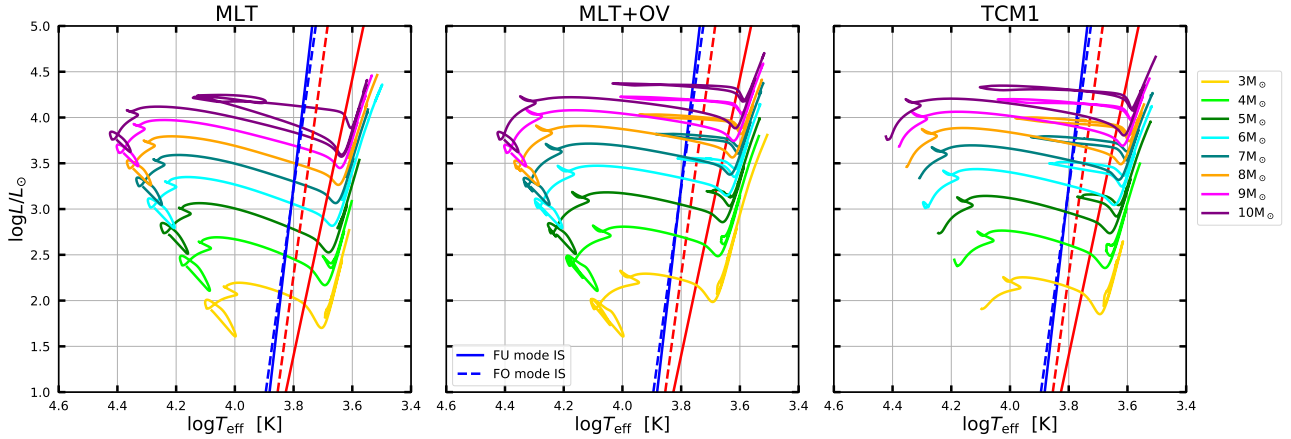


Figure 1: The evolutionary tracks for $(3-10)M_{\odot}$ from ZAMS to core helium burning phase computed using GARSTEC. The solid/dashed blue and red line represents the fundamental/first overtone blue and red edges of IS, respectively, computed using the Modules for Experiments in Stellar Astrophysics - Radial Stellar Pulsation (MESA-RSP) code.

Grevesse & Noels (1993). This gave $\alpha_{\text{MLT}}=1.75$ and $\alpha_{\text{TCM1}}=1.11$ for the model with MLT and the model with the TCM1, respectively (Teresa Braun, private communication).

The TC parameters for the TCM1 are: α_{TCM1} , α_{ω} , α_s , and C_D . The values of these TC parameters used for the TCM1 are listed in Table 1.

2.2 Stellar evolutionary models

In this work, we compute two different sets of models. We first do a comparative study of the evolutionary tracks of Cepheids in terms of the different convection approaches. The second set of models is computed to compare with the observations of the detached eclipsing binaries. For the first set, we computed the evolutionary tracks for the mass range $(3-10)M_{\odot}$ in intervals of $1M_{\odot}$ from the zero-age main sequence (ZAMS) up to the core helium-burning phase. The tracks were computed using the MLT alone, MLT with exponential overshooting as outlined in Freytag et al. (1996), and subsequently, the TCM1. The diffusive overshooting introduced by Freytag et al. (1996) models overshooting with a mixing profile which decreases exponentially as a function of the distance to the Schwarzschild boundary. The initial models for the TCM1 were selected from the MLT plus exponential overshooting evolutionary tracks at the onset of the main-sequence phase following Ahlborn et al. (2022).

We adopted the OPAL equation of state and OPAL opacities (Iglesias & Rogers, 1996), supplemented by low-temperature tabular opacity data from Ferguson et al. (2005). For the results presented in Section 3.1, we have chosen the mass fractions of hydrogen $X = 0.70$, helium $Y = 0.28$, and metals $Z = 0.02$ assuming the scaled solar abundance determined by Grevesse & Noels (1993). We adopted the default GARSTEC parameter values for all other parameters. The overshooting in the models using MLT plus ad-hoc overshooting is controlled by the parameter f_{OV} , for which we also adopted the default parameter, which is $f_{OV} = 0.02$. This parameter was calibrated by fitting GARSTEC-isochrones to the color-magnitude diagrams of open clusters (Magic et al., 2010). For the MLT and MLT plus overshoot calculations, the calibrated solar mixing length parameter was $\alpha_{\text{MLT}} = 1.75$, while for the TCM1 approach, it was $\alpha_{\text{TCM1}} = 1.11$ (as described in Section 2.1).

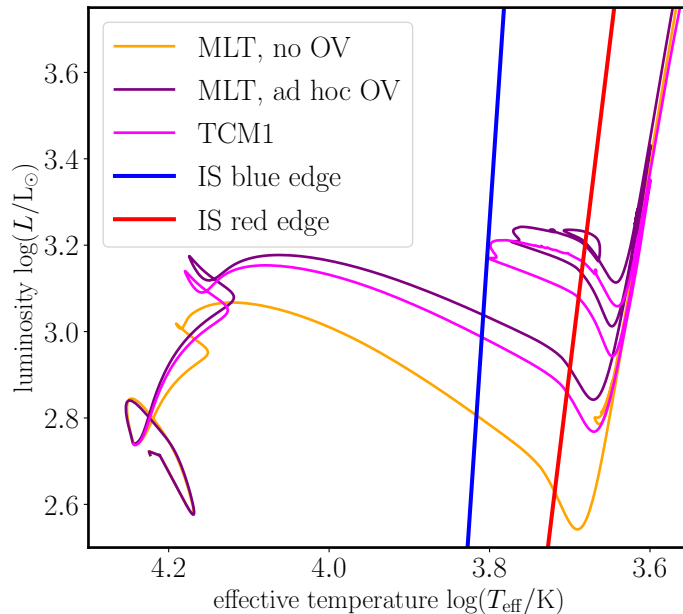


Figure 2: The evolutionary tracks for a $5M_{\odot}$ from ZAMS to core helium burning phase computed using GARSTEC. The blue and red line represents the fundamental blue and red edges of IS, respectively, computed using the MESA-RSP code.

For the results presented in Section 3.2, we used the same α_{TCM1} . The parameters different from the first set-up are the initial masses and metallicities (adopted based on the literature) which we will mention in the corresponding section specific to each system. To convert $[\text{Fe}/\text{H}]$ to X, Y, Z , we have used the following: primordial helium $Y_{\text{P}} = 0.2485$ (Hinshaw et al., 2013), He-enrichment ratio $\frac{dY}{dZ} = 1.4$ (Cassisi & Salaris, 2011) and $\frac{Z}{X_{\odot}} = 0.0244$ (Grevesse & Noels, 1993).

3 Results

3.1 Comparison to MLT

The resulting tracks for $(3 - 10)M_{\odot}$ are displayed in Fig. 1 along with the Cepheid instability strip (IS) edges. The Cepheid blue and red IS edges plotted in Fig. 1 and 2 are taken from Deka et al. (in preparation). For a clear visual comparison, the evolutionary track for a $5M_{\odot}$ with MLT only, MLT with ad-hoc overshooting and TCM1 are presented in Fig. 2, highlighting the differences among the three tracks. It becomes apparent that the MLT approach alone fails to reproduce the blue loops of Cepheids, which was previously achieved through the introduction of ad-hoc overshooting. Remarkably, the TCM1 has accomplished this without necessitating fine-tuning of the involved numerical parameters. The notable difference is that the overall luminosity increases for the tracks with MLT with ad-hoc overshooting and TCM1 as compared to that with MLT only, thereby reducing the mass discrepancy. The upper panel of Fig. 3 displays the turbulent kinetic energy (TKE) profile as a function of fractional mass for an evolutionary model of a $5M_{\odot}$ star computed using the TCM1. The TKE profile

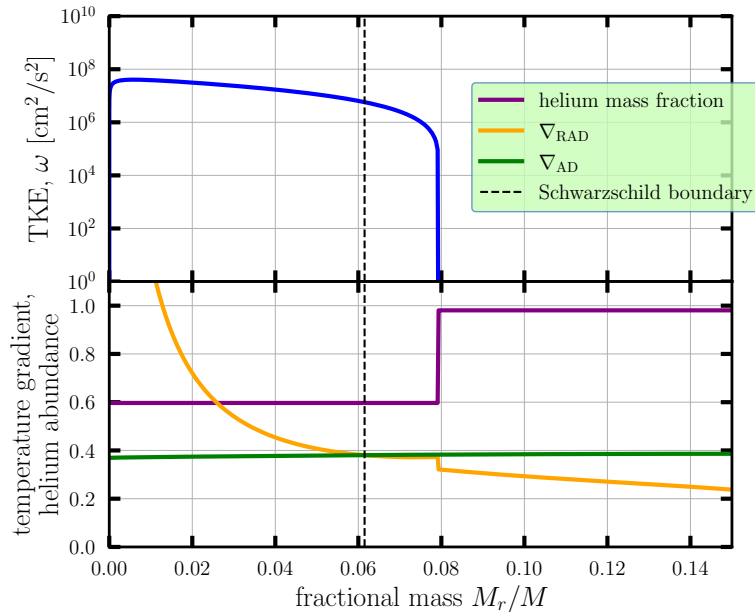


Figure 3: The upper panel shows the turbulent kinetic energy profile as a function of fractional mass for an evolutionary model of a $5M_{\odot}$ star computed using the TCM1. The TKE profile is obtained for a model with central helium abundance of $Y_c = 0.6$. The lower panel shows the Schwarzschild boundary (black dashed line) and the helium profile (purple line). We determine the Schwarzschild boundary as the point where $\nabla_{\text{ad}} = \nabla_{\text{rad}}$. The orange and green lines indicate the radiative ∇_{rad} and adiabatic ∇_{ad} temperature gradients, respectively.

is obtained for a model with central helium abundance of $Y_c = 0.6$. The lower panel of Fig. 3 shows the Schwarzschild boundary and the helium profile. We determine the Schwarzschild boundary as the point where $\nabla_{\text{ad}} = \nabla_{\text{rad}}$. It can be seen that the convective core is extended beyond the Schwarzschild boundary, which has been achieved without additional prescription of overshooting.

3.2 Comparison to observations

For a more comprehensive comparison between the evolutionary model computed using the TCM1 and observations, we selected five eclipsing binary systems from Pilecki et al. (2018). These systems consist of at least one companion which is a Cepheid. All these systems are detached (Pilecki et al., 2018), hence single evolutionary tracks will be suitable for modeling the individual components. The stellar parameters obtained from binary modeling and important for this study are listed in Table 3. The input parameters adopted for each system are mentioned in their corresponding subsections. However, we utilized the same radiative mass-loss rates from Reimers (1975, 1977), employing a factor of $\eta = 0.25$ for all the systems. The obtained results are summarized in Table 2. We have obtained the measured final parameters from the tracks using minimum χ^2 -values in RT_{eff} -plane for each component of the binary systems. It is also important to note that we are only presenting three of these systems within the scope of this report and plan to work on the remaining systems in the future.

3.2.1 OGLE-LMC-CEP-0227

OGLE-LMC-CEP-0227 is the first classical Cepheid that was spectroscopically confirmed to be a member of an eclipsing binary system, and for which the dynamical masses and other physical parameters were determined (Pietrzyński et al., 2010). Pilecki et al. (2013) estimated the fundamental properties of the system with significantly improved precision as compared to Pietrzyński et al. (2010). They found the mass of the Cepheid (the “primary”) to be slightly higher than that of the non-pulsating companion (“secondary”), but within the errors this mass hierarchy is not conclusive. Since Pilecki et al. (2018) in a re-analysis of the orbital solution claim that the mass of the companion is indeed lower than that of the Cepheid ($4.06 \pm 0.03 M_{\odot}$ vs. $4.15 \pm 0.03 M_{\odot}$), we adopted the values by Pilecki et al. (2013) for a first set of models (see Table 2), contrary to what others have done before (for example Cassisi & Salaris, 2011; Prada Moroni et al., 2012), assuming that the secondary in fact has a slightly lower mass.

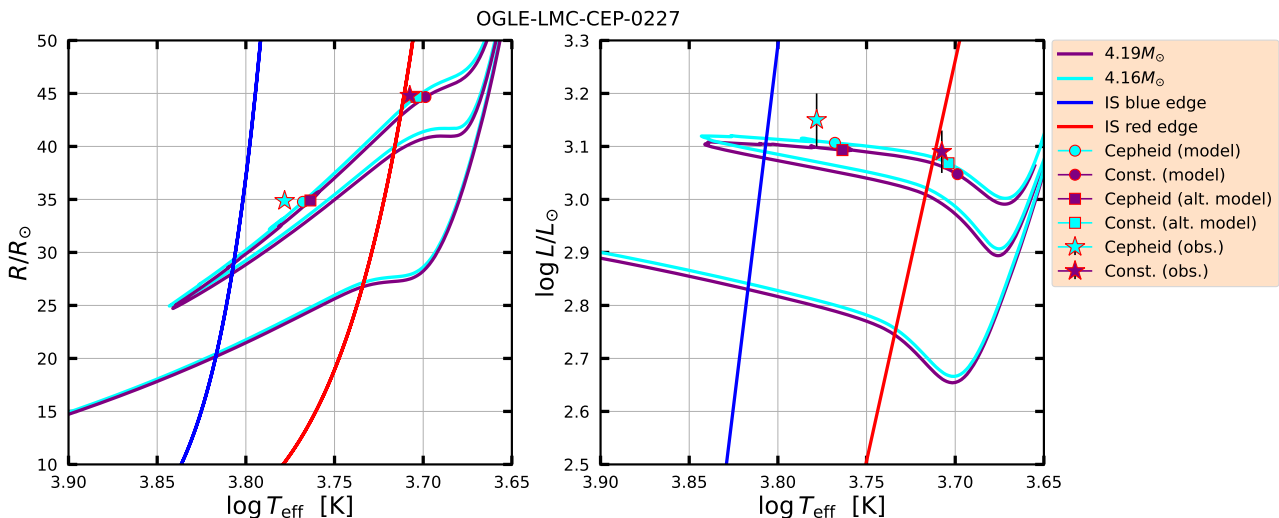


Figure 4: The evolutionary tracks for OGLE-LMC-CEP-0227 computed using TCM1. The left panel shows the tracks in radius–effective temperature (RT_{eff}) plane, while the right panel shows them in the luminosity–effective temperature (LT_{eff}) plane. The observed parameters for the system are plotted over the tracks with the colored stars. The modeled parameters are plotted with colored circles, while the alternative model parameters are shown in colored rectangles (for reference, see Table 2). The error bars are smaller than the symbols in the (RT_{eff}) plane.

Additionally, we selected slightly higher initial masses than their current dynamical masses, in order to account for the mass lost in previous evolutionary phases. The adopted metallicity for these calculations is $[\text{Fe}/\text{H}] = -0.5$ dex (Pilecki et al., 2018). The tracks obtained are shown in Fig. 4. The left panel shows the tracks in $R - T_{\text{eff}}$ plane, while the right panel shows it in $L - T_{\text{eff}}$ plane. Both sets of evolutionary tracks consistently predict effective temperatures, luminosities, and radii that agree with the observed values. The Cepheid component occupies the Cepheid IS, whereas the non-pulsating companion is outside the IS.

While our models nicely reproduce the location in the HRD for both components, with the selected mass values the evolutionary state of the stars is inconsistent, because the secondary (of lower mass, but same age) appears to be further evolved. This contradicts basic stellar physics, and was probably the reason why other teams used an inverted mass ratio. We followed this

approach as well and assigned tentatively the higher mass to the secondary, and the lower one to the Cepheid. The parameters of the resulting models that now reproduce the observed locations in the diagrams of Fig. 4 are also given in Table. 2 under the label of “alternative model”. Now, the locations along the tracks are consistent with the more massive star being already in a more advanced phase of evolution. The inconsistency is now shifted to the observers, suggesting that their mass assignment may be erroneous.

An alternative solution of the problem could be of theoretical nature. For the original mass assignments, one could assume that the luminosity of our models might be too low by about 0.1 dex, and therefore both the ad hoc overshooting approach and our TCM1 model are both underestimating the size of the mixed core. In this case (shifting the tracks in Fig. 4 upwards), the Cepheid would lie on the lower blue loop branch, while the less massive non-pulsating companion would be close to entering it from the red.

In conclusion, even this system, which has been modelled several times in the literature, is not free of open questions, still posing challenges to both observers and theorists.

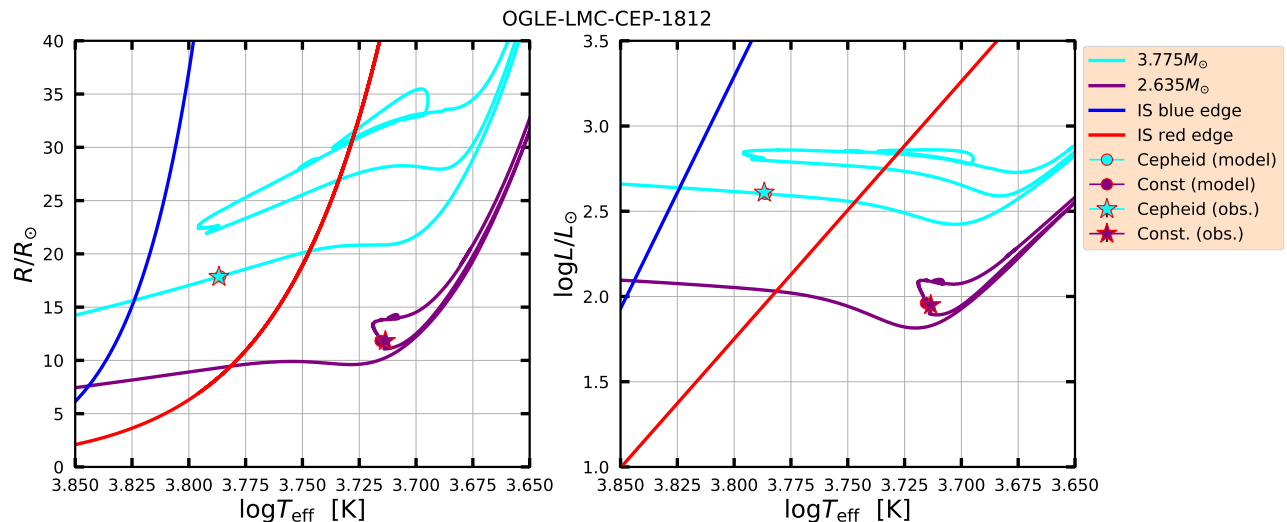


Figure 5: The same as Fig. 4 but for OGLE-LMC-CEP-1812 system. The error bars are smaller than the symbols.

3.2.2 OGLE-LMC-CEP-1812

OGLE-LMC-CEP-1812 is the second classical Cepheid existing in an eclipsing binary system. The metallicity is taken to be $[\text{Fe}/\text{H}] = -0.33$ dex (Pietrzyński et al., 2011). The initial masses used for the primary and secondary companion are $3.8M_{\odot}$ and $2.775M_{\odot}$, respectively. The tracks are displayed in Fig. 5. Interestingly, we find the Cepheid in the first crossing of the IS, which is a rare phenomenon as typically only a few percent of the Cepheids should be found at this stage (Neilson et al., 2012). This is because the intermediate-mass and massive stars evolve on a thermal timescale after they exhaust the hydrogen in their cores (cf. Gautschi, 2022). However, the possibility of finding a Cepheid in the first crossing of the IS is still there, even though less likely. Also, another crucial aspect of this system is that the less massive companion appears to be more evolved than the Cepheid. Neilson et al. (2015) also modeled this system using MLT plus overshooting. They also found that the Cepheid is located on

the first crossing of the IS and that the companion is further evolved than the more massive Cepheid implying that both stars reach their observed radii for different ages. One explanation put forward for this age anomaly is that this system originally was a triple system, and the Cepheid evolved from the merger of two main-sequence stars. Another possible explanation is that the observed age difference could be attributed to mass transfer between the binary system's two components. More investigation is needed to put constraints on this. However, we note that the scope of this project is to test the TCM1. We find that again we obtain the same result with the TCM1 as the typical MLT plus overshooting approach, and that our results are consistent with [Neilson et al. \(2015\)](#).

3.2.3 OGLE-LMC-CEP-4506

We have computed the stellar tracks for each of the stars in the OGLE-LMC-CEP-4506 system with masses $3.625M_{\odot}$ and $3.535M_{\odot}$, and mass fractions of hydrogen $X = 0.737$, helium $Y = 0.258$ and metals $Z = 0.005$. This corresponds to an $[\text{Fe}/\text{H}]$ of -0.56 dex. The chemical composition is adopted from [Gieren et al. \(2015a\)](#). Fig. 6 shows the computed tracks. Here, we see that both the Cepheid and the non-pulsating star are inside the IS. [Gieren et al. \(2015b\)](#) modeled this system using MLT plus overshooting and found a similar result. This occurs as the observed temperature is too high to situate the non-pulsating component outside the IS. However, due to the very long orbital period of 1550 days for this binary system, acquiring well-distributed spectroscopic data presents a significant challenge. Further observations are needed for this system to put constraints on its stellar parameters ([Pilecki et al., 2018](#)).

We also find that the evolutionary tracks computed with the TCM1 underpredict the luminosities and radii of both components, even though the remaining discrepancy with the observations is much smaller as compared to computation with MLT without overshooting. The remaining discrepancy could be resolved by increasing the non-local parameter α_{ω} of the TCM1 which would increase the convective core size on the main sequence and in turn lead to a higher luminosity in the core helium burning phase (Fig.B.2 in [Ahlborn et al., 2022](#)). Additionally, we computed tracks using a different $[\text{Fe}/\text{H}] = -0.5$ dex (as used for the other two binary systems) which leads to a larger mismatch between the models and observation (see Fig. 7). Hence, decreasing the metallicity could also increase the agreement between the model and observations. Given the current constraints on the metallicity, it is difficult to determine whether a different value of α_{ω} is really needed or whether the mismatch is just an effect of an incorrect metallicity. Considering the assumptions of the TCM1, we expect the same TC parameter values to apply to different systems. We note that computations with MLT plus ad-hoc overshooting lead to a slightly better agreement between the evolutionary tracks and the observations (see Fig. 8) due to a larger convective core size on the main sequence (see [Ahlborn et al. \(2022\)](#), their Fig. 7). The remaining difference between MLT plus ad-hoc overshooting and the TCM is however much smaller than compared to MLT without overshooting as mentioned before.

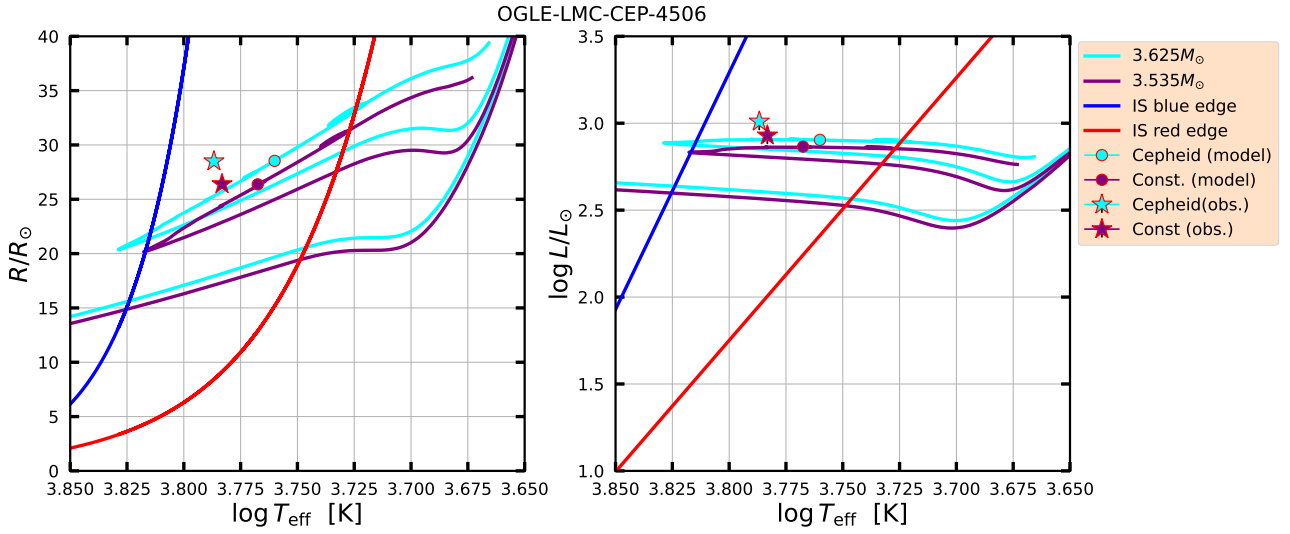


Figure 6: The same as Fig. 4 but for OGLE-LMC-CEP-4506 system. The error bars are smaller than the symbols.

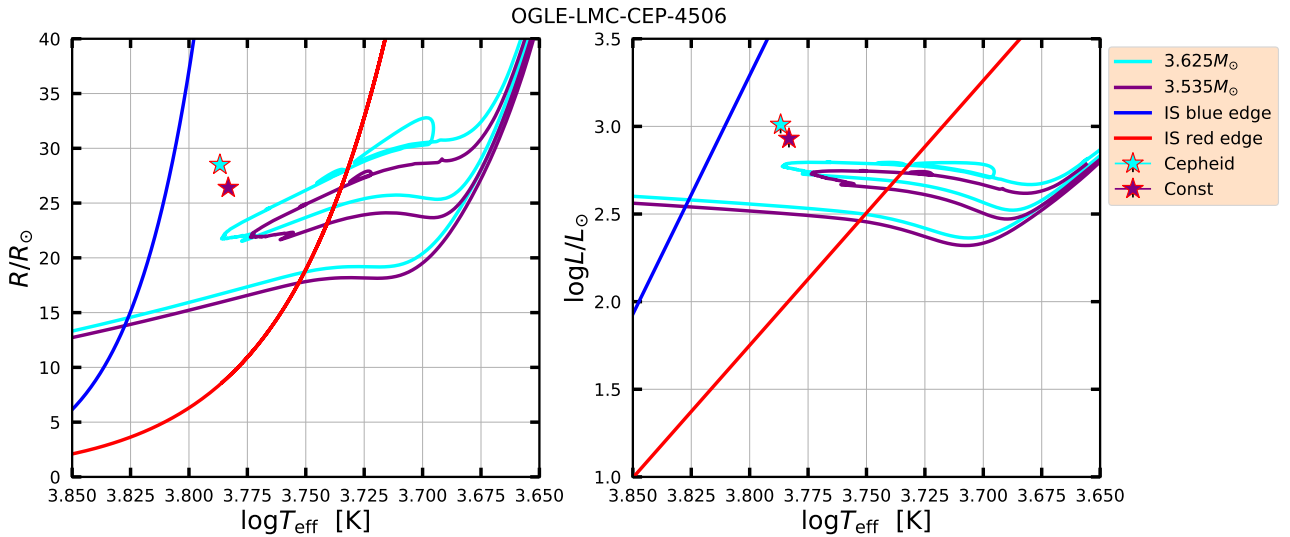


Figure 7: Same as Fig. 6 but with a different metallicity, $[\text{Fe}/\text{H}] = -0.5$ dex.

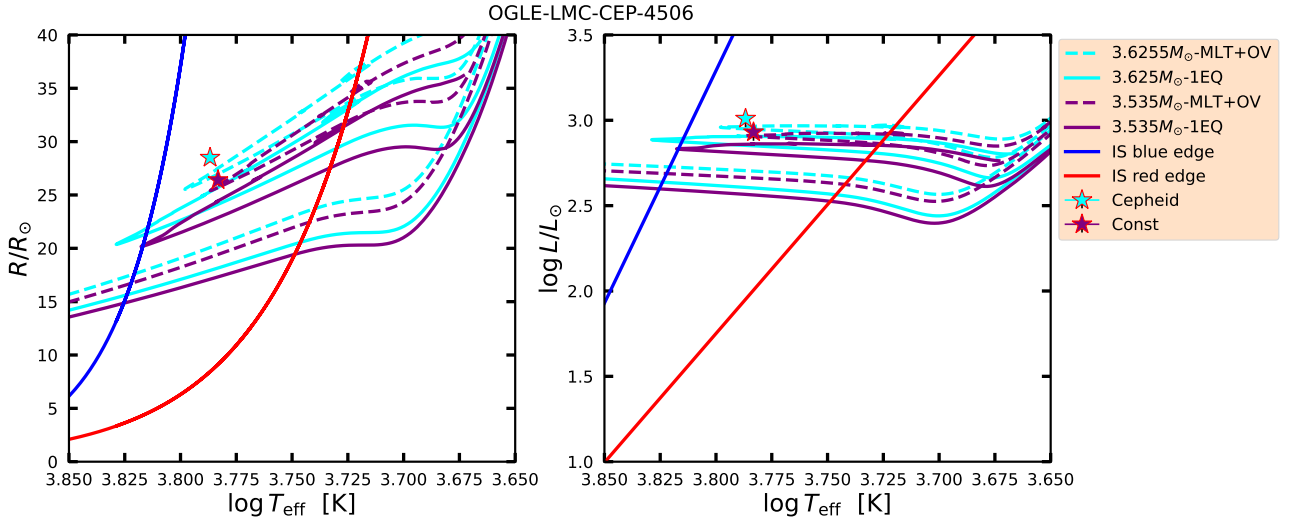


Figure 8: The same as Fig. 6 for OGLE-LMC-CEP-4506 system with additional tracks computed with MLT plus overshooting (dashed line). The metallicity adopted is $[\text{Fe}/\text{H}] = -0.56$ dex. The error bars are smaller than the symbols.

Table 2: The stellar parameters obtained for the binary components from the evolutionary tracks are listed below. The subscripts p and s refer to the primary and secondary components, respectively.

OGLE ID	Parameters	Initial ^a	Final ^b	Observations
OGLE LMC-CEP-0227	M_p/M_\odot	4.19	4.18	4.165 ± 0.032
	M_s/M_\odot	4.16	4.15	4.134 ± 0.037
	R_p/R_\odot		34.77	34.92 ± 0.29
	R_s/R_\odot		44.66	44.85 ± 0.34
	L_p/L_\odot		3.10	3.158 ± 0.049
	L_s/L_\odot		3.04	3.097 ± 0.047
	$T_{\text{eff},p}$ (K)		5859	6050 ± 160
	$T_{\text{eff},s}$ (K)		4997	5120 ± 130
	age _p (Myr)		157.6	
	age _s (Myr)		161.1	
	$[\text{Fe}/\text{H}]$	-0.5 dex		
	η	0.25		
OGLE LMC-CEP-0227 (“alternative model”)	M_p/M_\odot	4.16	4.15	4.165 ± 0.032
	M_s/M_\odot	4.19	4.18	4.134 ± 0.037
	R_p/R_\odot		34.90	34.92 ± 0.29
	R_s/R_\odot		44.67	44.85 ± 0.34
	L_p/L_\odot		3.09	3.158 ± 0.049
	L_s/L_\odot		3.06	3.097 ± 0.047
	$T_{\text{eff},p}$ (K)		5802	6050 ± 160
	$T_{\text{eff},s}$ (K)		5055	5120 ± 130
	age _p (Myr)		160.2	
	age _s (Myr)		158.2	

Continued on the next page

	[Fe/H]	−0.5 dex		
	η	0.25		
OGLE LMC-CEP-1812	M_p/M_\odot	3.775	3.76	3.76 ± 0.03
	M_s/M_\odot	2.635	2.62	2.62 ± 0.02
	R_p/R_\odot		17.87	17.85 ± 0.13
	R_s/R_\odot		11.83	11.83 ± 0.08
	L_p/L_\odot		2.60	2.61 ± 0.04
	L_s/L_\odot		1.96	1.95 ± 0.04
	$T_{\text{eff,p}}(\text{K})$		6112	6120 ± 150
	$T_{\text{eff,s}}(\text{K})$		5195	5170 ± 120
	age _p (Myr)		181.2	
	age _s (Myr)		493.8	
		[Fe/H]	−0.33 dex	
	η	0.25		
OGLE LMC-CEP-4506	M_p/M_\odot	3.625	3.62	3.61 ± 0.03
	M_s/M_\odot	3.535	3.53	3.52 ± 0.03
	R_p/R_\odot		28.54	28.5 ± 0.2
	R_s/R_\odot		26.37	26.4 ± 0.2
	L_p/L_\odot		2.90	3.01 ± 0.05
	L_s/L_\odot		2.86	2.93 ± 0.05
	$T_{\text{eff,p}}(\text{K})$		5755	6120 ± 160
	$T_{\text{eff,s}}(\text{K})$		5854	6070 ± 150
	age _p (Myr)		213.2	
	age _s (Myr)		225.8	
		[Fe/H]	−0.55 dex	
	η	0.25		

^a Initial parameters considered to compute the evolutionary tracks

^b Obtained parameters from the computed evolutionary tracks

4 Summary and Conclusions

The ‘‘Cepheid mass discrepancy’’ has long been a challenging puzzle in astrophysics. One proposed solution that has been put forward to solve this discrepancy concerns the size of the convective core. Previously, this had been addressed by incorporating overshooting in an ad-hoc manner. In this study, we have treated the convective core overshooting using a more physically motivated theory of convection. Our analysis showed that the evolutionary tracks computed using MLT with overshooting and TCM1 exhibit the same features as shown in Fig. 1 and 2. The former one is incorporated in an ad-hoc manner and its parameters are calibrated to observations. The latter relies on a physically more realistic description of turbulent convection derived from the hydrodynamic equations. Furthermore, we compared the stellar models using TCM1 with observations of Cepheids in binary systems. From the three systems we used to test the TCM1, only OGLE-LMC-CEP-0227 works reasonably well. For the other two systems, we find similar problems in obtaining the correct values from the models as was reported for modeling efforts done with MLT plus overshooting. The Cepheid of the OGLE-LMC-CEP-1812

system is predicted to be in a very short-lived stellar evolutionary phase, which is not impossible but very unlikely. In OGLE-LMC-CEP-4506, there is a possibility of high uncertainty in estimating the effective temperature from observation due to the relatively long orbital period. At present, the MLT plus overshooting model seems to work better than the TCM1. In the future, a thorough parameter study of the free parameters of the TCM1 could help in improving the models to better match with observations and also find the ideal parameter set to use for stellar models. We will further extend this study by incorporating the other two binary systems OGLE-LMC-CEP-1718 and OGLE-LMC-CEP-2532 (Table 3). Furthermore, carrying out such a comparison as done in this work with the more physically complete TCM3 would be the next step towards better modeling of convection in stellar evolution codes.

Acknowledgements

We express our gratitude to the Kavli Foundation and the Max Planck Institute for Astrophysics for their support of the Kavli Summer Program in Astrophysics, 2023. This program provided the environment in which a significant portion of this project was undertaken.

References

- Ahlborn F., Kupka F., Weiss A., Flaskamp M., 2022, *A&A*, **667**, A97
- Anderson R. I., Ekström S., Georgy C., Meynet G., Mowlavi N., Eyer L., 2014, *A&A*, **564**, A100
- Biermann L., 1932, *ZAp*, **5**, 117
- Böhm-Vitense E., 1958, *ZAp*, **46**, 108
- Canuto V. M., 1992, *ApJ*, **392**, 218
- Canuto V. M., 1993, *ApJ*, **416**, 331
- Canuto V. M., 1997, *ApJ*, **482**, 827
- Canuto V. M., 2011, *A&A*, **528**, A76
- Canuto V. M., Dubovikov M., 1998, *ApJ*, **493**, 834
- Cassisi S., Salaris M., 2011, *ApJ*, **728**, L43
- Cox A. N., 1980, *ARA&A*, **18**, 15
- Ferguson J. W., Alexander D. R., Allard F., Barman T., Bodnarik J. G., Hauschildt P. H., Heffner-Wong A., Tamanai A., 2005, *ApJ*, **623**, 585
- Flaskamp M., 2003, PhD thesis, Technical University of Munich, Germany
- Freytag B., Ludwig H. G., Steffen M., 1996, *A&A*, **313**, 497
- Gautschy A., 2022, *arXiv e-prints*, p. arXiv:2209.11502

Gieren W., et al., 2015a, [ApJ](#), **815**, 28

Gieren W., et al., 2015b, [ApJ](#), **815**, 28

Grevesse N., Noels A., 1993, [Physica Scripta Volume T](#), **47**, 133

Hinshaw G., et al., 2013, [ApJS](#), **208**, 19

Iglesias C. A., Rogers F. J., 1993, [ApJ](#), **412**, 752

Iglesias C. A., Rogers F. J., 1996, [ApJ](#), **464**, 943

Keller S. C., 2008, [ApJ](#), **677**, 483

Kuhfuß R., 1986, [A&A](#), **160**, 116

Kuhfuß R., 1987, PhD thesis, Technical University of Munich, Germany

Kupka F., Ahlborn F., Weiss A., 2022, [A&A](#), **667**, A96

Li Y., Yang J. Y., 2007, [MNRAS](#), **375**, 388

Magic Z., Serenelli A., Weiss A., Chaboyer B., 2010, [ApJ](#), **718**, 1378

Neilson H. R., Cantiello M., Langer N., 2011, [A&A](#), **529**, L9

Neilson H. R., Langer N., Engle S. G., Guinan E., Izzard R., 2012, [ApJ](#), **760**, L18

Neilson H. R., Izzard R. G., Langer N., Ignace R., 2015, [A&A](#), **581**, L1

Pietrzyński G., et al., 2010, [Nature](#), **468**, 542

Pietrzyński G., et al., 2011, [ApJ](#), **742**, L20

Pilecki B., et al., 2013, [MNRAS](#), **436**, 953

Pilecki B., et al., 2018, [ApJ](#), **862**, 43

Prada Moroni P. G., Gennaro M., Bono G., Pietrzyński G., Gieren W., Pilecki B., Graczyk D., Thompson I. B., 2012, [ApJ](#), **749**, 108

Reimers D., 1975, *Memoires of the Societe Royale des Sciences de Liege*, **8**, 369

Reimers D., 1977, [A&A](#), **61**, 217

Stellingwerf R. F., 1982, [ApJ](#), **262**, 330

Stobie R. S., 1969, [MNRAS](#), **144**, 485

Weiss A., Schlattl H., 2008, [Ap&SS](#), **316**, 99

Wuchterl G., 1995, [Computer Physics Communications](#), **89**, 119

Xiong D.-r., 1978, [Chinese Astronomy](#), **2**, 118

Xiong D.-R., 1986, [A&A](#), **167**, 239

A Stellar parameters for the binary systems considered in this work

The stellar parameters of the binary systems obtained from the literature are given in Table 3. We have chosen five of the systems described by [Pilecki et al. \(2013\)](#) and [Pilecki et al. \(2018\)](#) to test the TCM1 and have included them in the table. However, due to time constraints only three, OGLE-LMC-CEP-0227, OGLE-LMC-CEP-1812, and OGLE-LMC-CEP-4506 were modelled so far. The systems OGLE-LMC-CEP-1718 and OGLE-LMC-CEP-2532 are included here for completeness and will be studied in the future.

Table 3: Properties of the eclipsing binary systems obtained from the literature. “F” and “FO” denote the fundamental mode and first-overtone mode of Cepheids , respectively.

OGLE ID	Parameter	Primary	Secondary
OGLE-LMC-CEP-0227 (F) Source: Pilecki et al. (2013)	Orbital period (days)	309.404	
	Pulsation period (days)	3.797	...
	M/M_{\odot}	4.165 ± 0.032	4.134 ± 0.037
	R/R_{\odot}	34.92 ± 0.29	44.85 ± 0.34
	L/L_{\odot}	3.158 ± 0.049	3.097 ± 0.047
	$T_{\text{eff}}(\text{K})$	6050 ± 160	5120 ± 130
OGLE-LMC-CEP-1812 (F) Source: Pilecki et al. (2018)	Orbital period (days)	551.8	
	Pulsation period (days)	1.313	...
	M/M_{\odot}	3.76 ± 0.03	2.62 ± 0.02
	R/R_{\odot}	17.85 ± 0.13	11.83 ± 0.08
	L/L_{\odot}	2.61 ± 0.04	1.95 ± 0.04
	$T_{\text{eff}}(\text{K})$	6120 ± 150	5170 ± 120
OGLE-LMC-CEP-4506 (F) Source: Pilecki et al. (2018)	Orbital period (days)	1550	
	Pulsation period (days)	2.988	...
	M/M_{\odot}	3.61 ± 0.03	3.52 ± 0.03
	R/R_{\odot}	28.5 ± 0.2	26.4 ± 0.2
	L/L_{\odot}	3.01 ± 0.05	2.93 ± 0.05
	$T_{\text{eff}}(\text{K})$	6120 ± 160	6070 ± 150
OGLE-LMC-CEP-1718 (FO+FO) Source: Pilecki et al. (2018)	Orbital period (days)	412.8	
	Pulsation period (days)	1.964	2.481
	M/M_{\odot}	4.27 ± 0.04	4.22 ± 0.04
	R/R_{\odot}	27.8 ± 1.2	33.1 ± 1.3
	L/L_{\odot}	3.04 ± 0.06	3.18 ± 0.06
	$T_{\text{eff}}(\text{K})$	6310 ± 150	6270 ± 160
OGLE-LMC-CEP-2532 (FO) Source: Pilecki et al. (2018)	Orbital period (days)	800.4	
	Pulsation period (days)	2.035	...
	M/M_{\odot}	3.98 ± 0.10	3.94 ± 0.09
	R/R_{\odot}	29.2 ± 1.4	38.1 ± 1.8
	L/L_{\odot}	3.10 ± 0.06	2.84 ± 0.09
	$T_{\text{eff}}(\text{K})$	6350 ± 150	4800 ± 220